Samarium: magnetic neutron spectroscopic intensities

1993 J. Phys.: Condens. Matter 5 7269

(http://iopscience.iop.org/0953-8984/5/39/014)

Samarium: magnetic neutron spectroscopic intensities

Ewald Balcar† and Stephen W Lovesey‡

† Atomic Institute of the Austrian Universities, A-1020 Vienna, Austria
‡ Rutherford Appleton Laboratory, Didcot, Oxfordshire, OX11 0QX, UK

Received 13 May 1993

Abstract. The present work, while specific to samarium and motivated by recent neutron beam results, also serves to illustrate the largely unexpected richness of neutron electron spectroscopy and its potential for future development as a tool in studies of magnetic materials. In our calculation we have modelled samarium as a trivalent, isolated magnetic ion and we consider the dependence of the twelve states lowest in energy on the spin–orbit interaction strength. We then calculate the wavevector dependence of the inelastic structure factors for intra- and inter-multiplet magnetic neutron scattering from the ground state. For ease of comparison with experimental data an intensity profile for a sample incident neutron energy is given.

1. Introduction

The availability of beams of energetic neutrons produced in modern spallation sources has opened a host of exciting experimental opportunities for the investigation of magnetic substances. In fact, previously inaccessible inelastic transitions between atomic levels separated by 1 eV, or more, are now the subject of magnetic neutron scattering experiments. This new area of neutron spectroscopy complements and extends the information gained from optical experiments. Two main additional attractive features of neutron spectroscopy are the presence of transitions other than those in the dipole selection rules, and no hindrance in the study of bulk metallic properties.

The potential promise of neutron beam techniques to provide spectroscopic data for atoms in bulk magnetic materials has been convincingly demonstrated in the past few years. Energy level schemes for several rare earth and actinide atoms have been established with good accuracy. In the seminal experiment Williams *et al* [1] investigated samarium in its trivalent state and measured the wavevector dependence of the first inelastic transition at 130 meV from the ground state $^6H_{5/2}$ to $^6H_{7/2}$. Even with the high intensity of a pulsed spallation source the experiment proved to be very difficult due to the strong neutron absorption encountered in natural samarium.

Attention has now shifted to the more challenging and rewarding aspects of intrinsic line widths and intensities, and their interpretation in terms of atomic processes. On this issue, it is perhaps surprising just how sensitive intensities are to details of the atomic wavefunctions. This feature has recently been highlighted by us [2] in a study of the intensity profile for Pr.

Recently a new attempt to measure inelastic neutron scattering from samarium has been started by Needham *et al* [3] and this has prompted us to make a more complete theoretical analysis of the samarium spectrum, which encompasses interesting features well within the extended energy scale accessible by inelastic spallation neutron scattering.

We investigate transitions from the ground state to other levels, even levels of a different term, ^6F. Since the term energies are determined by the Coulomb interaction, we will refer to

0953-8984/93/397269+08$07.50

inter-term transitions also as Coulomb transitions while transitions within the levels split by spin–orbit interaction, intra-term transitions, will also be described as spin–orbit transitions.

New data emerging from current experiments certainly reflect some of the features predicted by theory but, hampered by strong neutron absorption, these data are as yet inconclusive with respect to detailed properties of the atomic states. The wavevector dependence of the intensities for the various possible inelastic transitions of Sm^{3+} derived from the theory of magnetic neutron scattering should serve as a guideline for the design of further experiments.

Thus, an outcome of the theoretical work reported here is an argued case for further work over the same energy scale but with better statistics. The latter can be achieved with today's instrumentation but an isotopically enriched sample, with very modest neutron absorption, is probably essential.

2. Energy levels of samarium (Sm^{3+})

In order to obtain a proper starting point for the introduction of the spin–orbit interaction we first have to consider the level structure resulting from the Coulomb interaction in the configuration f^5. Due to the large number of states in this configuration, the Russel–Saunders classification by the corresponding S, L-values is insufficient, as some of the terms of multiplicity two appear up to seven times, etc. in the level scheme. In total we find 73 Russel–Saunders terms of which the two lowest, ^{6}H and ^{6}F, which constitute our main focus of interest, are well separated in energy from the other states.

We have calculated the Coulomb energies of all levels by diagonalizing the Coulomb interaction for all multiply appearing S, L-combinations. The matrix elements of the Coulomb interaction were taken from the tables of Nielson and Koster [4]. We have used the numerical values for the Slater integrals $F^{(2,4,6)}$ (for Sm^{3+} doped into LaF_3) given by Carnall *et al* [5].

These energy levels are now subject to the spin–orbit interaction, which combines S and L to a total angular momentum J, with $|L-S| \leqslant J \leqslant L+S$. However, S and L are no longer exact quantum numbers because all states of the same value J are weakly coupled through the spin–orbit interaction.

With our intent to consider the two terms lowest in energy and their splitting into multiplets via spin–orbit interaction, we have restricted our calculations to those values of J, $J = \frac{1}{2}, \frac{3}{2}, \ldots \frac{15}{2}$, which are present in ^{6}H or ^{6}F. This corresponds to 10, 21, 28, 30, 29, 26, 20, 16 states with quantum numbers $J = \frac{1}{2}, \frac{3}{2}, \frac{5}{2}, \frac{7}{2}, \frac{9}{2}, \frac{11}{2}, \frac{13}{2}, \frac{15}{2}$, respectively.

The task of calculating the matrix elements of the spin–orbit interaction $\mathcal{H}_{SO}$ is facilitated by the use of Racah algebra [6], and the theory has been given in [7, 8] in more detail. The application of the Wigner–Eckart theorem to a scalar operator leads to

$$(vSLJM|\mathcal{H}_{SO}|v'S'L'J'M') = (-1)^{J-M}\begin{pmatrix} J & 0 & J \\ -M & 0 & M \end{pmatrix}(vSLJ||\mathcal{H}_{SO}||v'S'L'J)\delta_{JJ'}\delta_{MM'}. \quad (1)$$

The reduced matrix element appearing in (1) is proportional to the reduced matrix element of a unit tensor operator $W^{(1,1)0}$, see [7],

$$(vSLJ||\mathcal{H}_{SO}||v'S'L'J) = 6\sqrt{7/2}(vSLJ||W^{(1,1)0}||v'S'L'J). \quad (2)$$

The evaluation of this quantity is described by Judd [9] and requires the knowledge of the fractional parentage coefficients, for all terms involved, as tabulated in [4].

After diagonalization of the spin–orbit interaction for states of constant J we obtain the variation in energy for spin–orbit strengths $0 \leqslant \zeta \leqslant 200$ meV given in figure 1. A vertical line at $\zeta = 146$ meV indicates the spin–orbit strength listed by Carnall *et al* [5]. We note, however, that the neutron measurements of Williams *et al* and Needham *et al* [1, 3] put the first excited level $^6H_{7/2}$ at 130 meV above the ground state, which corresponds to a spin–orbit strength $\zeta \simeq 160$ meV in figure 1. If this latter value is taken as the basis of further calculations a level structure, given in table 1, emerges for Sm^{3+} (free ion).

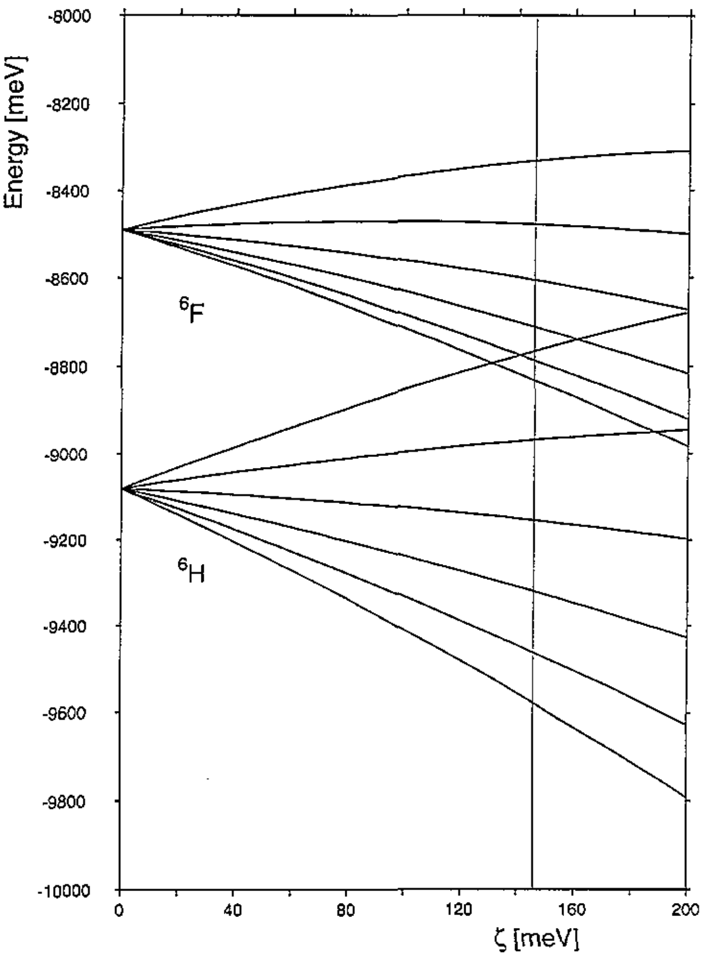

Figure 1. Energy dependence of the J-multiplets arising from ^6H and ^6F with the spin–orbit interaction for ζ up to 200 meV. The line is at 146 meV. Calculations reported in the text are for $\zeta = 160$ meV.

3. Magnetic intensities

One of the advantages of a magnetic neutron scattering experiment rests in the determination

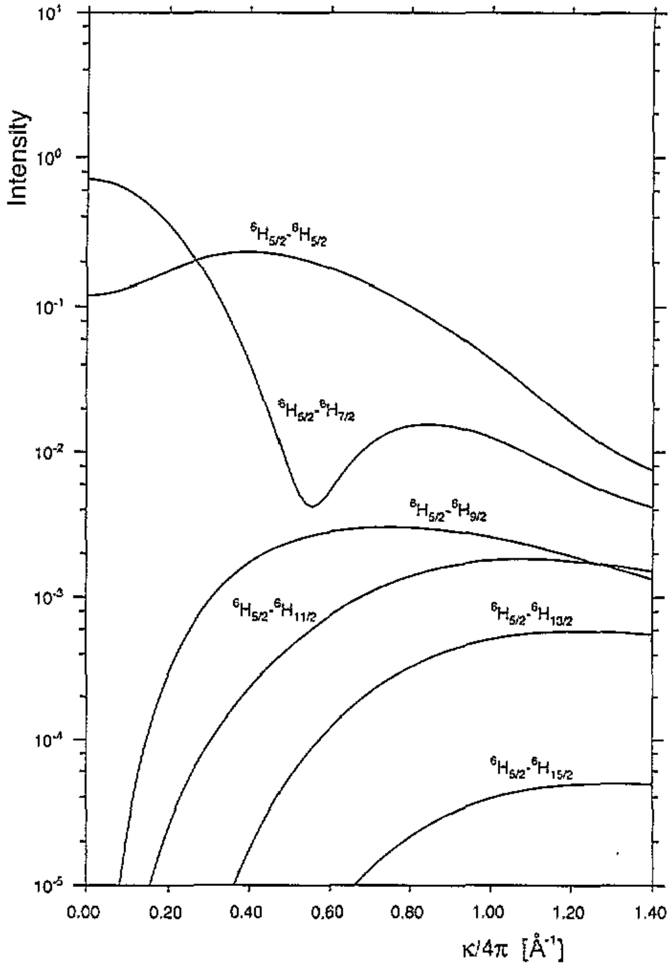

Figure 2. Magnetic neutron scattering intensity plotted as function of $\kappa/4\pi$ for elastic scattering and intra-term transitions. Note the logarithmic scale for the intensity. Attention is drawn to the unusual shape of the elastic atomic form factor, with a maximum away from the forward direction, and the pronounced dip in the structure factor for the dipole allowed transition. The latter has not been convincingly demonstrated in the published experimental data.

of the dependence of the cross-section on the change in the wavevector of neutrons participating in an inelastic event which is inherently governed by the properties of the atomic wavefunctions. In the following section we consider the intensities of inelastic transitions between the ground state, $^6H_{5/2}$ and the states listed in the table 1. Those magnetic scattering intensities and their wavevector (κ) dependence are described by a structure factor $\mathcal{G}(\kappa, \lambda, \lambda')$ as defined in

$$\frac{\mathrm{d}^2\sigma}{\mathrm{d}\Omega\,\mathrm{d}E'} = r_0^2 \frac{k'}{k} \mathcal{G}(\kappa, \lambda, \lambda')\delta(\hbar\omega - E_{\lambda'} - E_{\lambda}). \tag{3}$$

Here, $r_0 = (\gamma e^2/m_e c^2)$ is the usual measure of magnetic scattering, $\boldsymbol{\kappa} = \boldsymbol{k} - \boldsymbol{k}'$, with $\boldsymbol{k}$, $\boldsymbol{k}'$ and λ, λ' referring to the initial and final neutron wavevectors and target states, respectively. The theory related to the calculation of $\mathcal{G}(\kappa, \lambda, \lambda')$ has been covered in detail

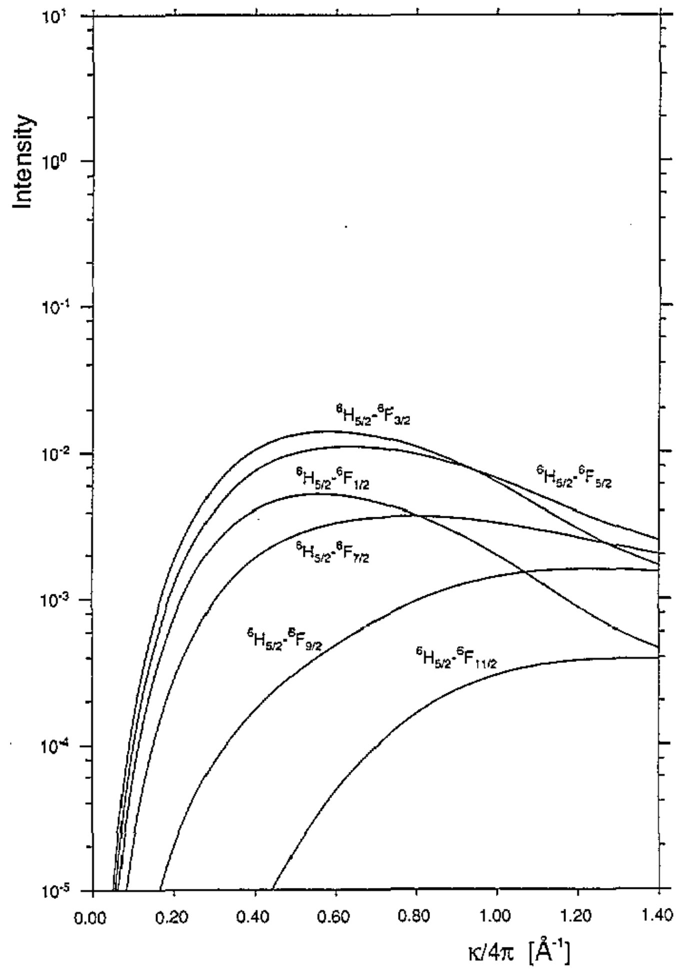

Figure 3. Magnetic neutron scattering intensity plotted as function of $\kappa/4\pi$ for inter-term transitions. By their very nature, none of these transitions is allowed by the dipole selection rule and hence all structure factors vanish in the forward direction of scattering.

in the literature, see [8, 10]. The numbers listed in table 2 describe the magnetic scattering cross section averaged over the directions of $\boldsymbol{\kappa}$ and they express the magnetic intensities for the various transitions through averages $\langle j_K \rangle$ of spherical Bessel functions

$$\langle j_K(\kappa) \rangle = \int_0^\infty \mathrm{d}r\, r^2\, R_l^2(r)\, j_K(\kappa r) \tag{4}$$

calculated with radial parts $R_l(r)$ of f-electron wavefunctions. The κ-dependence of magnetic scattering intensities is thus determined both by the coefficients listed in table 2 and the κ-dependence of the $\langle j_K \rangle$.

For a numerical evaluation of magnetic intensities we have used analytical expansions for the $\langle j_K \rangle$ derived from non-relativistic Hartree–Fock calculations [11, 12]. As the refinements on the confrontation between theory and experiment continue, one issue that needs to be addressed is the influence of relativistic corrections to the radial integrals.

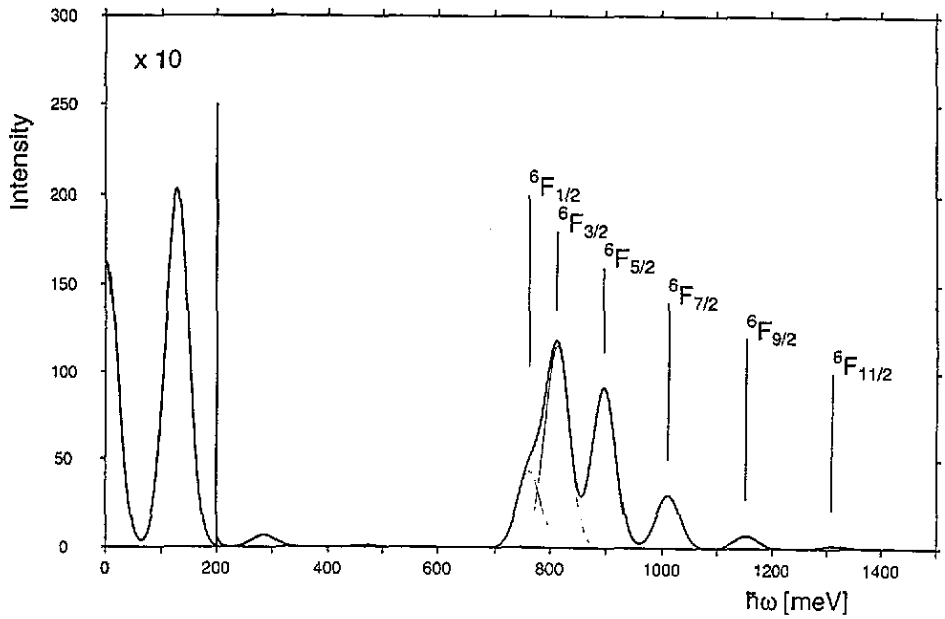

Figure 4. A calculated neutron spectrum given as a function of energy transfer $\hbar\omega$ for neutrons with a sample incident energy of 2500 meV. A scattering angle of 5° is assumed and the theoretical results have been folded with a Gaussian of FWHM (full width at half maximum) = 60 meV to account for a typical instrument resolution. The intensity below 200 meV has been reduced by a factor of 10 for convenience in graphical display. This figure combines the information contained in figures 1, 2 and 3 but does not aim to represent a real experiment.

Table 1. Energy differences between the ground state $^6H_{5/2}$ and some excited levels of Sm^{3+} with a spin–orbit interaction of $\zeta = 160$ meV.

Transition	(meV)
$^6H_{5/2} \rightarrow {}^6H_{7/2}$	128
$^6H_{5/2} \rightarrow {}^6H_{9/2}$	285
$^6H_{5/2} \rightarrow {}^6H_{11/2}$	468
$^6H_{5/2} \rightarrow {}^6H_{13/2}$	671
$^6H_{5/2} \rightarrow {}^6H_{15/2}$	892
$^6H_{5/2} \rightarrow {}^6F_{1/2}$	762
$^6H_{5/2} \rightarrow {}^6F_{3/2}$	812
$^6H_{5/2} \rightarrow {}^6F_{5/2}$	896
$^6H_{5/2} \rightarrow {}^6F_{7/2}$	1011
$^6H_{5/2} \rightarrow {}^6F_{9/2}$	1152
$^6H_{5/2} \rightarrow {}^6F_{11/2}$	1310

In figure 2 we display the wavevector dependence of the magnetic intensities for spin–orbit transitions between the ground state of Sm^{3+} and the states of the same ^6H multiplet listed in the upper part of table 1. The graphs correspond to the values given in table 2. We note the remarkable κ-dependence of the first inelastic transition to the state $^6H_{7/2}$ and the rapid decrease in intensity with the transition to $^6H_{15/2}$ being lowest by almost four orders of magnitude.

Figure 3 outlines the wavevector dependence of the Coulomb transitions from the ground

Table 2. Spherical average of the cross section for magnetic scattering inducing intra- and inter-multiplet transitions from the ground state of Sm^{3+} expressed through radial averages of spherical Bessel functions $\langle j_K \rangle$. Those numbers which are zero due to the properties of the magnetic scattering operator have no entry in the table.

	$\langle j_0\rangle^2$	$\langle j_0\rangle\langle j_2\rangle$	$\langle j_2\rangle^2$	$\langle j_2\rangle\langle j_4\rangle$	$\langle j_4\rangle^2$	$\langle j_4\rangle\langle j_6\rangle$	$\langle j_6\rangle^2$
				Samarium : Sm^{3+}			
$^6H_{5/2}$	0.119	1.291	3.518	0.046	0.040	−0.013	0.005
$^6H_{7/2}$	0.714	−1.387	0.750	0.059	0.110	−0.067	0.017
$^6H_{9/2}$			0.045	0.008	0.182	−0.003	0.091
$^6H_{11/2}$			0.004	−0.001	0.091	0.055	0.241
$^6H_{13/2}$					0.011	0.014	0.128
$^6H_{15/2}$					0.000	0.000	0.013
$^6F_{1/2}$			0.116	0.043	0.007	0.000	0.000
$^6F_{3/2}$			0.276	0.196	0.068	0.000	0.000
$^6F_{5/2}$			0.181	0.203	0.165	0.062	0.091
$^6F_{7/2}$			0.040	0.067	0.130	0.040	0.253
$^6F_{9/2}$			0.003	0.006	0.033	−0.012	0.394
$^6F_{11/2}$			0.000	0.000	0.002	−0.004	0.113

state to the multiplet states of ^6F. Most of the graphs are, unfortunately, rather smooth and show no marked variations in intensity.

Finally, in figure 4 the theoretical results are displayed for an incident neutron energy of 2500 meV. The peak at 130 meV has been observed by Williams *et al* [1]. The new spectral features around 800 meV arise from inter-term (Coulomb) transitions induced by magnetic neutron scattering. Inelastic intensity at these energies is present in the available experimental data [3], but in truth another study with better statistics is required for comparison with our calculation.

Although we have tried to use realistic values for the parameters used in the calculation, the intensity given in figure 4 does not aim to fully represent a real experiment. A number of essential experimental factors, such as the highly resonant character of the absorption of incident and outgoing neutrons, the instrumental luminosity, or a possible isotopic enrichment of the sample have not been included for the simple reason that such factors are peculiar to the specific arrangement adopted for an experiment.

4. Discussion

Recent experiments [3] on the inelastic magnetic scattering from samarium have motivated us to calculate a sample intensity profile for comparison. However, analysis of the present experimental data allows no definite conclusions to be drawn, since the neutron absorption cross section shows some variation in the critical energy region. Thus, although inelastic intensity is shown by the data, the physical origin is difficult to establish.

We have investigated the wavevector dependence of the magnetic neutron scattering from samarium for inter- and intra-term transitions. In view of anticipated experiments we can say that, except for the first excited level, the levels of the ground term multiplet will be very weak. Around 800 meV a group of levels belonging to the ^6F multiplet should be discernible in magnetic neutron scattering.

The line positions and intensities depend on atomic parameters, such as the spin–orbit coupling, and the influence of the concentrated environment, including strong electron correlations, can reasonably be deduced and compared with theoretical calculations. In this respect, samarium is of particular interest because it is a constituent in mixed valence materials, which show properties characteristic of a strong admixture of two or more f configurations in the ground state.

At present, the mixing of states with the same J has not been included in the theory. This could be done if and when there is demand for the satisfactory interpretation of experimental data. Future experiments, with an isotopically enriched sample for preference, should also aim to achieve a convincing confirmation of the striking features in the dipole structure factor.

Acknowledgments

The interest of A D Taylor and W G Williams is gratefully acknowledged.

References

[1] Williams W G, Boland B C, Bowden Z A, Taylor A D, Culverhouse S and Rainford B D 1987 *J. Phys. F: Met. Phys.* **17** L151
[2] Balcar E and Lovesey S W 1991 *Proc. Int. Conf. Neutron Scattering Physica* B **180 &181** 182
[3] Needham L M, Williams W G, Taylor A D 1993 *J. Phys.: Condens. Matter* **5** 2591
[4] Nielson C W and Koster G F 1963 *Spectroscopic Coefficients for the* p^n, d^n *and* f^n *Configurations* (Cambridge, MA: MIT Press)
[5] Carnall W T, Goodman G L, Rajnak K and Rana R S 1989 *J. Chem. Phys.* **90** 3443
[6] Racah G 1943 *Phys. Rev.* **63** 171
[7] Balcar E and Lovesey S W 1992 *J. Phys.: Condens. Matter* **4** 2271
[8] Osborn R, Balcar E, Lovesey S W and Taylor A D 1991 *Handbook of Physics and Chemistry of Rare Earths* vol 14, ed K A Gschneidner and L R Eyring (Amsterdam: North-Holland)
[9] Judd B R 1963 *Operator Techniques in Atomic Spectroscopy* (New York: McGraw-Hill)
[10] Balcar E and Lovesey S W 1989 *Theory of Magnetic Neutron and Photon Scattering* (Oxford: University Press)
[11] Lisher E J and Forsyth J B 1971 *Acta Crystallogr.* A **27** 545
[12] Blume M, Freeman A J and Watson R E 1962 *J. Chem. Phys.* **37**